

Remote sensing investigation of inundation, elevation and land use assessment for vulnerability analysis in Moscow, Russia

K Choudhary¹, M S Boori^{1,2} and A Kupriyanov^{1,3}

¹Samara National Research University, Moskovskoye Shosse34, Samara, Russia, 443086

²American Sentinel University, 2260 South Xanadu Way, Suite 310, Aurora, Colorado, USA

³Image Processing Systems Institute - Branch of the Federal Scientific Research Centre "Crystallography and Photonics" of Russian Academy of Sciences, Molodogvardeyskaya str. 151, Samara, Russia, 443001

Abstract. Land use/cover change analysis assists decision makers to ensure sustainable development and to understand the dynamics of our changing environment. This research work is to understand natural and environmental vulnerability situation and its cause such as intensity, distribution and socio-economic effect in the Moscow, Russia based on remote sensing and Geographical Information System (GIS) techniques. A model was developed by following thematic layers: vegetation, LULC, geology, geomorphology and soil in ArcGIS 10.2 software using multi-spectral satellite data. With increasing scientific and political interest in regional aspects of global environmental changes, there is a strong stimulus to better understand the patterns causes and environmental consequences of LULC expansion in the elevation of Moscow state, one of the areas in the nation with fast economic growth and high population density. Satellite remote sensing images (Landsat TM, ETM and OLI) were employed to detect land cover changes. A 70 to 300 m inundation land loss scenarios for surface water and sea level rise (SLR) were developed using digital elevation models of study site topography through remote sensing and GIS techniques by ASTER GDEM and Landsat OLI data. The most severely impacted sectors are expected to be the vegetation, wetland and the natural ecosystem. Improved understanding of the extent and response of SLR will help in preparing for adaptation.

1. Introduction

Russia has a largely continental climate because of its sheer size and compact configuration. Most of its land is more than 400 km. from the sea and the centre is 3,840 km. from the sea. Russia's mountain ranges, predominantly to the south and the east, block moderating temperatures from the Indian and Pacific Oceans but European Russia and northern Siberia lack such topographic protection from the Arctic and North Atlantic Oceans. Moscow located in European Russia. It's the area of high environment sensitivity zone due to harsh climate conditions with maximum time frozen temperature below then zero [1-2]. The region is drained by numerous rivers and dotted with lakes due to heavy rainfall. Numerous studies have been performed to understand the variations in the Land surface temperature as a result of changes in the land surface properties. Since the 1960s, scientists have extracted and modelled various vegetation biophysical variables using remote sensing data and the normalized difference vegetation index is one such widely adopted index. Inverse relationship has

been reported between land surface temperature and vegetation index. Nowadays, it is recognize that climate change and sea level rise will impact seriously upon the natural environment and human society in the area [3-4]. There for sea level rise has to be one of the main impacts of climate change in Moscow. Presently remote sensing and GIS techniques are the powerful tool to investigate, predict and forecast environmental change scenario in a reliable, non-invasive, rapid and cost effective way with considerable decision making strategies. The main aim of this research work is to describe natural hazards impacts and land loss due to water level inundation from 70 to 300m in Volga river basin located in Moscow [5-6].

Vulnerability is a function of exposure, sensitivity and adaptive capacity. Where potential impacts are a function of exposure and sensitivity hence, vulnerability is a function of potential impacts and adaptive capacity. Where exposure components characterize the stressors and the entities under stress; sensitivity components characterize the first order effects of the stresses. These measures can be quantitative (e.g. precipitation variability, distance to market) or qualitative (e.g. political party affiliation, environmental preservation ethic). Other slightly different view favoured by the hazards and disasters research community is that adaptive capacity consists of two subcomponents: coping capacity and resilience. Coping capacity is the ability of people and places to endure the harm and resilience is the ability to bounce back after exposure to the harmful events. In both cases, individuals and communities can take measures to increase their abilities to cope and bounce back; again depending on the physical, social, economic, spiritual and other resources they have or have access to. Another basic issue in this analysis work is to assign weights to each factor according to its relative effects of factors considered in the vulnerability in a thematic layer. The application of subjective weightings on the one hand gives us some indication of how the relative importance of different factors might change with context and can also tell us how sensitive vulnerability rating are to perceptions of vulnerability in the expert community.

2. Study Area

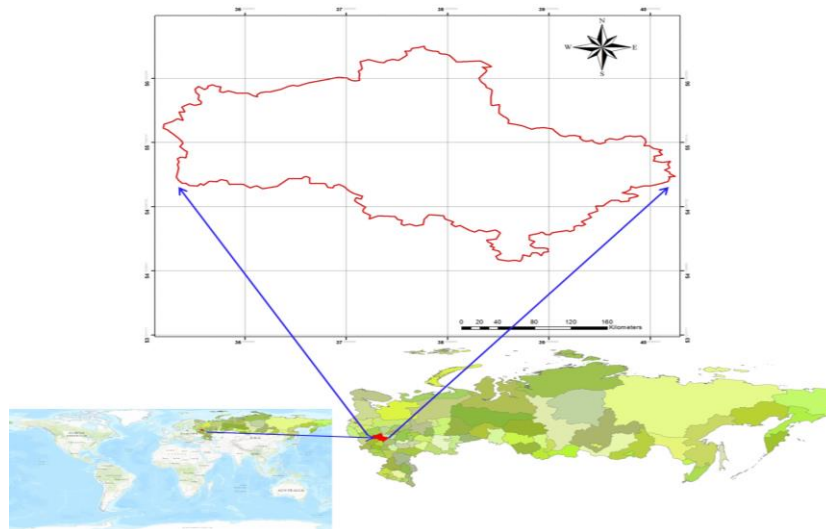


Figure 1. Location map of the study area in Moscow Region, Russia.

Moscow region an important historical, cultural, social and economic center in Russian Federation was selected for this study (fig.1). Moscow is the one of the most densely populated regions in the country and is the second most populated federal region. The Oblast has no official administrative center, it is public authorities are located in Moscow and across other locations in the Oblast. As of the 2010 Census, its population was 7,095,120 and 7,23,1068 recorded in the 2015 Census. The latitude of the city is $55^{\circ} 45' 7''$ N and longitude is $37^{\circ} 36' 56''$ E. The region is highly industrialized, such as metallurgy, oil refining, mechanical engineering, food, energy and chemical industries [7-8].

The climate of Moscow region is humid continental, short but warm summers and long cold winters. The average temperature is 3.5°C (38.3°F) to 5.5°C (41.9°F). The coldest months are

January and February average temperature of -9°C (16°F) in the west and -12°C (10°F) in the east. The minimum temperature is -54°C (-65°F). Here are more than three hundred rivers in Moscow regions and most rivers belong to the basin of the Volga [9]. Which itself only crosses a small part in the north of Moscow region. They are mostly fed by melting snow and the flood fall on April-May. The water level is low in summer and increases only with heavy rain [10-11]. The river freezes over from late November until April.

3. Data and Methodology

3.1. Data

In this research work we used primary (satellite data) and secondary data such as ground truth for land use/cover classes and topographic sheets. The ground truth data were collected using Global Positioning System (GPS) for the year of 2015 in the month of June to August for image analysis and classification accuracy [12-13]. The specific satellite images used were Landsat OLI (Operational Land Imager) for landscape and Advanced Space borne Thermal Emission and Reflection Radiometer (ASTER) Global Digital Elevation Model (ASTER GDEM) for elevation information.

3.2. Image pre-processing and classification

In pre-processing, first all images were georeferenced by WGS 1984 UTM projection, later on calibrated and remove there errors/dropouts. We use specific band combination and use image enhancement techniques such as histogram equalization to improve the classification accuracy [14]. At this stage, 50 points were selected as GCPs (Ground Control Points) for all images. Data sources used for the GCP selection were: digital topographic maps, GPS (Global Positioning Points) acquisitions. The data of ground truth were adapted for each single classifier produced by its spectral signatures for producing classification maps. For land use/cover classification, supervised maximum likelihood algorithm (MLC) was used in ArcGIS 10.2 software. MLC classification is based on training sites (signature) provided by the analyser based on his experience [15-16]. After training site whole image classified according to similar digital value of training site and finally classification give land use classified image of the area (fig.2). Seven main land use/cover classes have been find namely agriculture, barren land, forest, settlements, scrubland, water body and wetland in the study area (table. 1).

Table 1. Classes delineated on the basis of supervised classification.

Class name	Description
Agricultural	Cultivated areas, crop lands, grass lands, vegetables, fruits etc.
Barren land	This contains open lands mostly barren but also small vegetation.
Forest	Small trees and shrub vegetation area except for vegetation.
Scrubland	Scrub is a plant community describe by vegetation shrubs, often also including grasses and herbs.
Settlements	Includes construction activities along the coastal dunes as well as sporadic houses within the local village and some governmental buildings.
Water body	All the water within land mainly river, ponds, lakes etc.
Wetland	A wetland is a land area with standing water and low soil fertility.

A preparative requirement for the analysis of flooding impacts was the development of spatial datasets. A 1m spatial resolution digital elevation model (DEM) with error within 224 mm in elevation was constructed using ASTER GDEM images (fig.2). The GIS environment was used to classify and map the topology of land threatened by inundation [17].

The length of the sand spit at some places is more than 1km and they are highly vulnerable to river erosion basin.

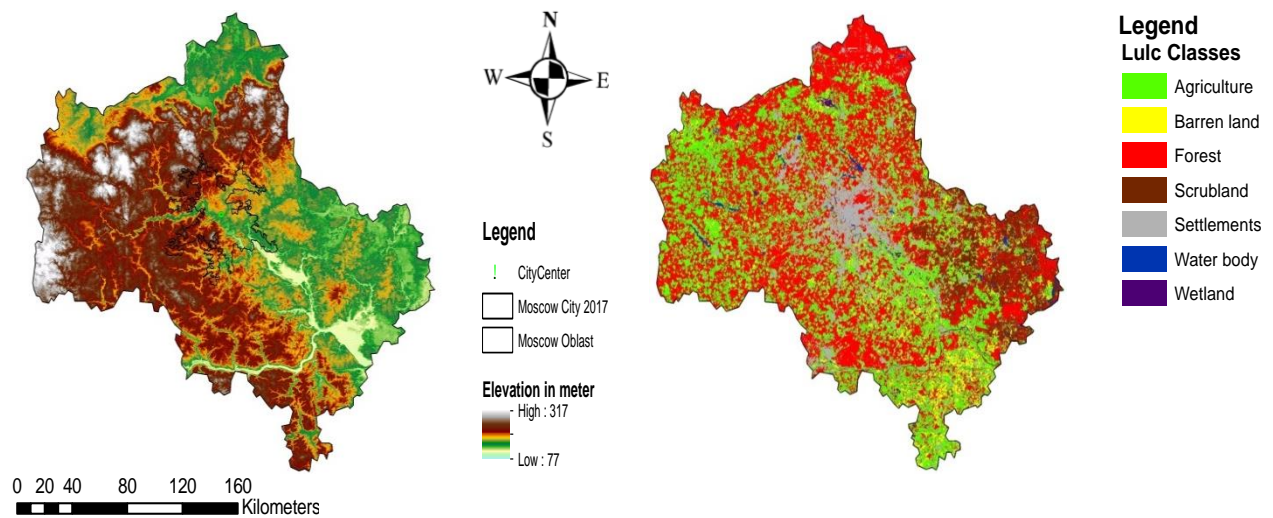


Figure 2. Elevation and land use/cover map of Moscow, Russia.

3.3. Data Analysis

All multi-spectral and temporal data were georeferenced based on topographic sheets with the help of ArcGIS 10.2 software. To improve the quality of research analysis we used different band ratio, image enhancement techniques and principal component analysis and in last supervised classification.

Table 2. Stability values of landscape units. (Ecodinamica Tricart, 1977).

Unit	Pedogenesis / morphogenesis Relation	Value
Stable	Prevails pathogenesis	1.0
Intermediate	Balance between pedogenesis and morphogenesis	2.0
Unstable	Prevails morphogenesis	3.0

Table 3. Weight table to each unite in a thematic layer.

Thematic maps/classes	Vulnerability grade levels
Land use/cover	
Agriculture	1.4
Barren land	1
Forest	1.7
Scrubland	2.2
Settlements	3
Water body	0.5
Wetland	0.8
Vegetation	
Dark coniferous forest	2.8
Grass	1.9
Grass herb	2
Oak forest	2.7
Pine	2.6
Pine leave forest	2.4
Shrub	2.3
Sphagnum bogs	1.6
Spruce	1.3
Wooded swampy fens	2.9
Geomorphology	
Plain area	2.5
Shrub land	2.3
Urban area	3
Water body	0.5
Wetland	0.8

Geology	
Flat	2.5
Gently undulating	2
Undulating	1.9
Soil	
Chernozems podzolized	1.9
Greys forest	2.1
Light-greys forest	1.8
Peats boggy	1.5
Podzols gleyic	1.4
Sod-podzolics	1.7
Sod-podzolics deepgley and gleyic	0.9

Thematic maps (fig. 3) of geology, geomorphology, soil, vegetation and land use/cover were prepared from Landsat ETM+ and OLI imageries. The weight of all landscape units based on Ecodinamica Tricart 1977 and Barbosa 1997 [18] stability concept, where stability was classified according to table 2. The weights of a landscape unit indicate the importance of any factor in relation to others. In natural vulnerability all thematic layer give same weight but in environmental vulnerability all thematic layer were given different weight based on their sensitivity in the study area.

The degree of vulnerability for all units was range from 0.0 to 3.0 (table 3) based on Barbosa and Crepani et al. (1996). The degree of vulnerability varies from 0 to 3 and is ranked as extreme, high, moderate, reasonable and low vulnerability. The weights of compensation indicate the importance of any factor in relation to others, as can be seen in the formula below for natural vulnerability map:

$$[(\text{Theme 1}) + (\text{Theme 2}) + (\text{Theme 3}) + (\text{Theme 4})] / 4$$

For environment vulnerability we use following formula:

$$0.2 \times [\text{Theme 1}] + 0.1 \times [\text{Theme 2}] + 0.1 \times [\text{Theme 3}] + 0.1 [\text{Theme 4}] + 0.5 \times [\text{Theme 5}]$$

Where: Theme 1: Geomorphology map, Theme 2: Simplified geological map, Theme 3: Soil map, Theme 4: Vegetation map and Theme 5: Land use/cover map.

The result mean was distributed in following five natural and environmental vulnerability classes:

1. Low vulnerability: less than or equal to 1.00;
2. Reasonable vulnerability: 1.1 to 1.50;
3. Moderate vulnerability: 1.51 to 2.00;
4. High vulnerability: 2.1 to 2.50;
5. Extreme vulnerability: greater than or equal to 2.51

4. Results

4.1. Land loss due to inundation

The DEM presented in figure 4 shows that low-lying land is more extensive at the north and center of the study area. The areas lower than 1m above mean sea level (MSL), which are at risk of inundation under the minimum inundation level are vegetation, industry and urban area basically whole city.

The main results of land loss due to inundation are presented in Figure 5. The most significant changes would occur south-east side of the Moscow.

At the minimum inundation level (70m in fig.4), 0.04% (20.24 km²) of the total area (table 4) would be flooded including: urban areas, natural vegetation and agricultural land and beaches. The area of submergence for 80m rise in water level is up to 60.12 km² (0.13%) and subsequently for 90m 258.29 km² (0.55%), 100m 895.84 km² (1.92%), 110m 2417.18 km² (5.18%), 120m 5108.59 km² (10.94%), 130m 8779.34 km² (18.80%), 140m 12815.38 km² (27.44%), 150m 16792.16 km² (35.95%), 180m 27976.67 km² (59.88%), 210m 38787.89 km² (82.98%), 240m 44584.13 km² (95.37%), 275m 46578.68 km² (99.62%) and 300m 46754.70 km² (100%) respectively (table 2). From the land use/cover map, it is clear that the maximum area is covered by agriculture which include Moscow city.

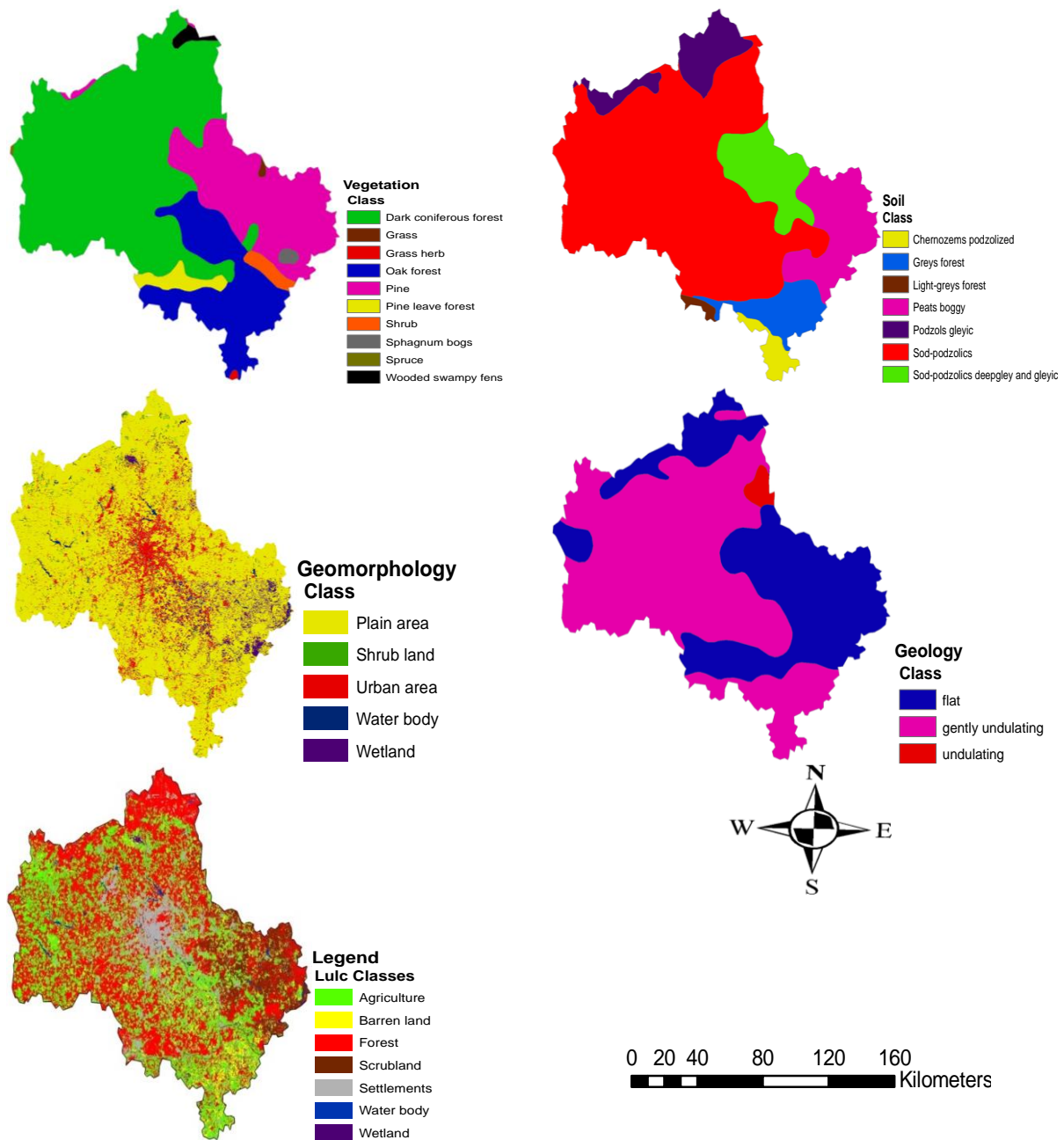


Figure 3. Simplified vegetation, soil, geomorphology, geology and land use/cover map.

At the full inundation level 300m in fig. Such a loss of land implies that the population living presently in these areas would be displaced. Even if some parts of the ecosystem of the wetland are not destroyed, because those parts could adapt to sea level rise and move landwards, the species richness is likely to decrease, due to repugnant new conditions where several plant communities and rare species would disappear. The area least vulnerable to inundation would be the southern and east part of the study area. However, parts of city and port, as well as an important river beach and natural forest would be flooded.

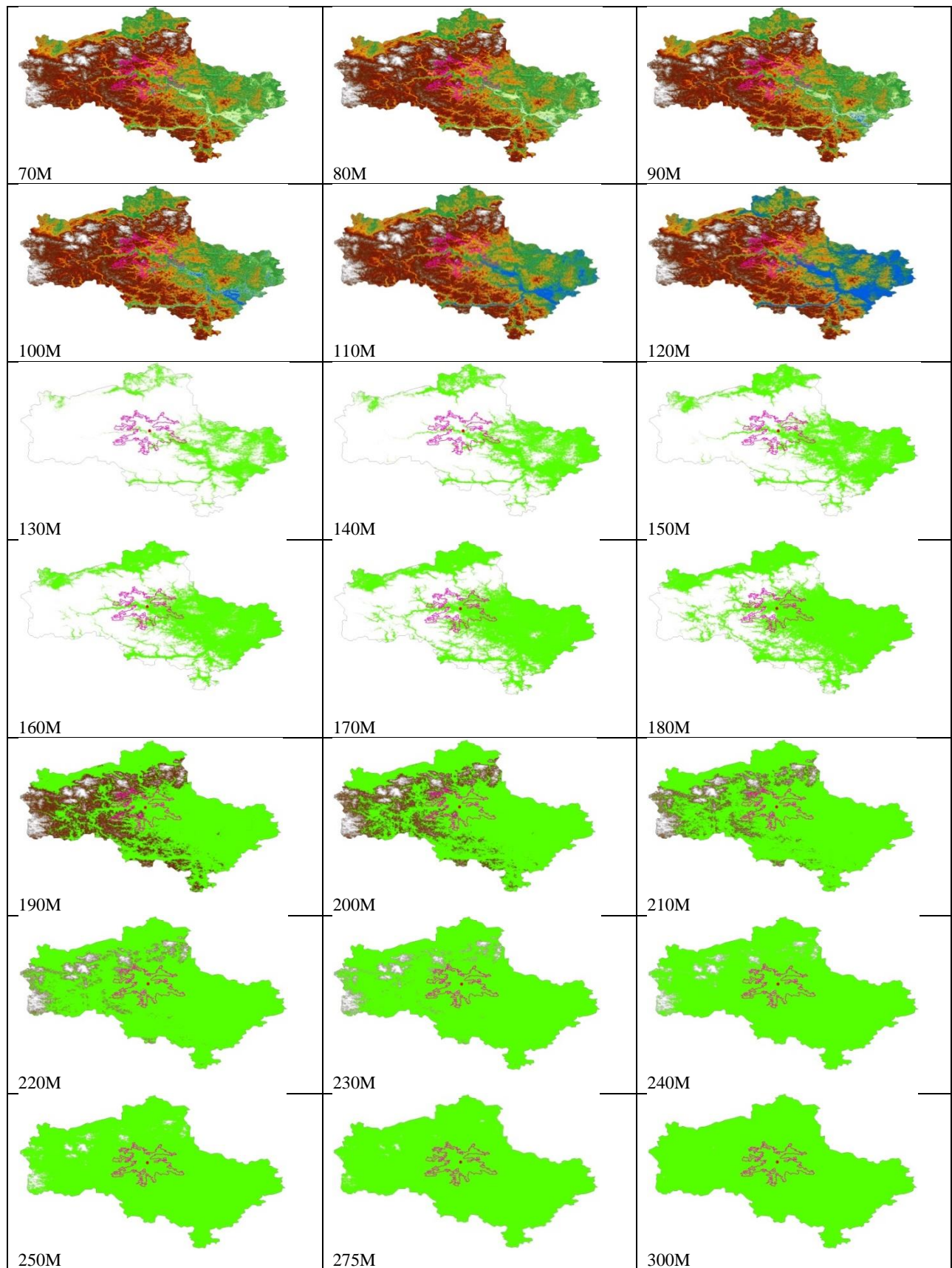


Figure 4. Land areas vulnerable to inundation in the Moscow, Russia.

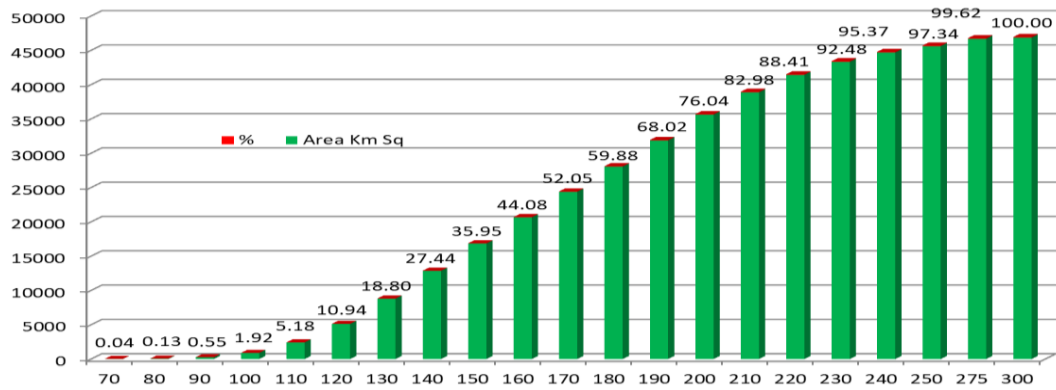


Figure 5. Inundation area graph of the Moscow, Russia.

Table 4. Potential land loss of the main sectors for 70m to 300m inundation levels scenarios (in km² and in % of the total inundated areas).

	70M		80M		90M		100M		110M		120M		130M	
Class name	km ²	%												
Agriculture	4.92	24.32	22.86	38.02	119.46	46.25	388.84	43.41	853.78	35.32	1581.83	30.96	2557.14	29.13
Barren land	2.35	11.62	6.56	10.91	27.79	10.76	99.96	11.16	285.46	11.81	564.95	11.06	866.86	9.87
Forest	3.38	16.68	9.33	15.52	37.41	14.48	123.66	13.80	364.95	15.10	1001.52	19.60	2184.16	24.88
Scrubland	6.18	30.54	12.33	20.51	39.49	15.29	157.59	17.59	549.33	22.73	1182.53	23.15	1812.09	20.64
Settlements	1.66	8.18	4.23	7.04	16.80	6.50	71.10	7.94	229.20	9.48	542.06	10.61	1031.46	11.75
Water body	1.30	6.41	3.69	6.14	12.58	4.87	36.90	4.12	90.60	3.75	143.23	2.80	186.29	2.12
Wetland	0.45	2.24	1.12	1.86	4.76	1.84	17.79	1.99	43.85	1.81	92.48	1.81	141.34	1.61
Total	20.24	0.04	60.12	0.13	258.29	0.55	895.84	1.92	2417.18	5.18	5108.59	10.94	8779.34	18.80
	140M		150M		160M		170M		180M		190M		200M	
Class name	km ²	%												
Agriculture	3605.91	28.14	4651.49	27.70	5722.11	27.79	6903.08	28.39	8202.99	29.32	9545.05	30.03	10772.92	30.31
Barren land	1159.12	9.04	1448.88	8.63	1724.89	8.38	2000.08	8.23	2266.48	8.10	2506.25	7.88	2689.91	7.57
Forest	3667.29	28.62	5188.49	30.90	6621.71	32.16	7975.34	32.80	9352.34	33.43	10959.28	34.48	12840.17	36.13
Scrubland	2363.85	18.45	2793.90	16.64	3072.01	14.92	3225.66	13.27	3291.92	11.77	3317.75	10.44	3332.07	9.38
Settlements	1627.70	12.70	2272.80	13.53	2939.31	14.27	3611.60	14.85	4225.56	15.10	4780.97	15.04	5198.22	14.63
Water body	219.43	1.71	240.84	1.43	299.20	1.45	370.93	1.53	394.77	1.41	418.45	1.32	431.27	1.21
Wetland	172.08	1.34	195.77	1.17	213.47	1.04	227.91	0.94	242.61	0.87	258.15	0.81	273.61	0.77
Total	12815.38	27.44	16792.16	35.95	20592.70	44.08	24314.60	52.05	27976.67	59.88	31785.89	68.02	35538.18	76.04
	210M		220M		230M		240M		250M		275M		300M	
Class name	km ²	%												
Agriculture	11770.03	30.34	12506.84	30.26	13040.38	30.16	13413.83	30.09	13655.11	30.01	13881.56	29.80	13902.42	29.73
Barren land	2813.50	7.25	2886.41	6.98	2933.22	6.78	2962.56	6.64	2980.15	6.55	2992.10	6.42	2992.95	6.40
Forest	14680.51	37.85	16235.11	39.28	17450.69	40.37	18331.89	41.12	18951.63	41.64	19740.06	42.38	19889.92	42.54
Scrubland	3342.19	8.62	3350.29	8.11	3357.22	7.77	3362.99	7.54	3368.20	7.40	3376.74	7.25	3377.19	7.22
Settlements	5459.78	14.08	5620.17	13.60	5716.00	13.22	5776.87	12.96	5815.11	12.78	5847.92	12.55	5851.71	12.52
Water body	437.79	1.13	441.77	1.07	444.10	1.03	445.60	1.00	446.68	0.98	449.23	0.96	449.42	0.96
Wetland	284.08	0.73	287.53	0.70	289.38	0.67	290.39	0.65	290.77	0.64	291.07	0.62	291.09	0.62
Total	38787.89	82.98	41328.12	88.41	43230.99	92.48	44584.13	95.37	45507.66	97.34	46578.68	99.62	46754.70	100.00

4.2. Vulnerability analysis

Natural and environmental vulnerability maps are shown relationship in between landscape and vulnerability and able to tackle answers such as comparing of different types of vulnerability zones in the study area.

4.3. Natural vulnerability

Its map shows that maximum area in safe zones as 56.91% area in moderate vulnerability and 20.10% area in reasonable vulnerability zones, which represent that around 78% area of total study area is safe zone. Around 11.70% area goes in high vulnerability which is really need proper management

otherwise it will increase and harmful. The low vulnerability area is only 5.44% of the total study area, which is present in river and water body area. 5.83% area has been under extreme vulnerability, which is very less and close to water bodies. High vulnerability is due to fluctuation and extreme climate condition. Maximum vegetation area and close to river basin area under moderate vulnerability zone. Some part of wetland and vegetation under reasonable vulnerability and low vulnerability area, which represent maximum safe area in this study area. It is low vulnerability area due to less socio-economic activities and high density of vegetation (fig.6).

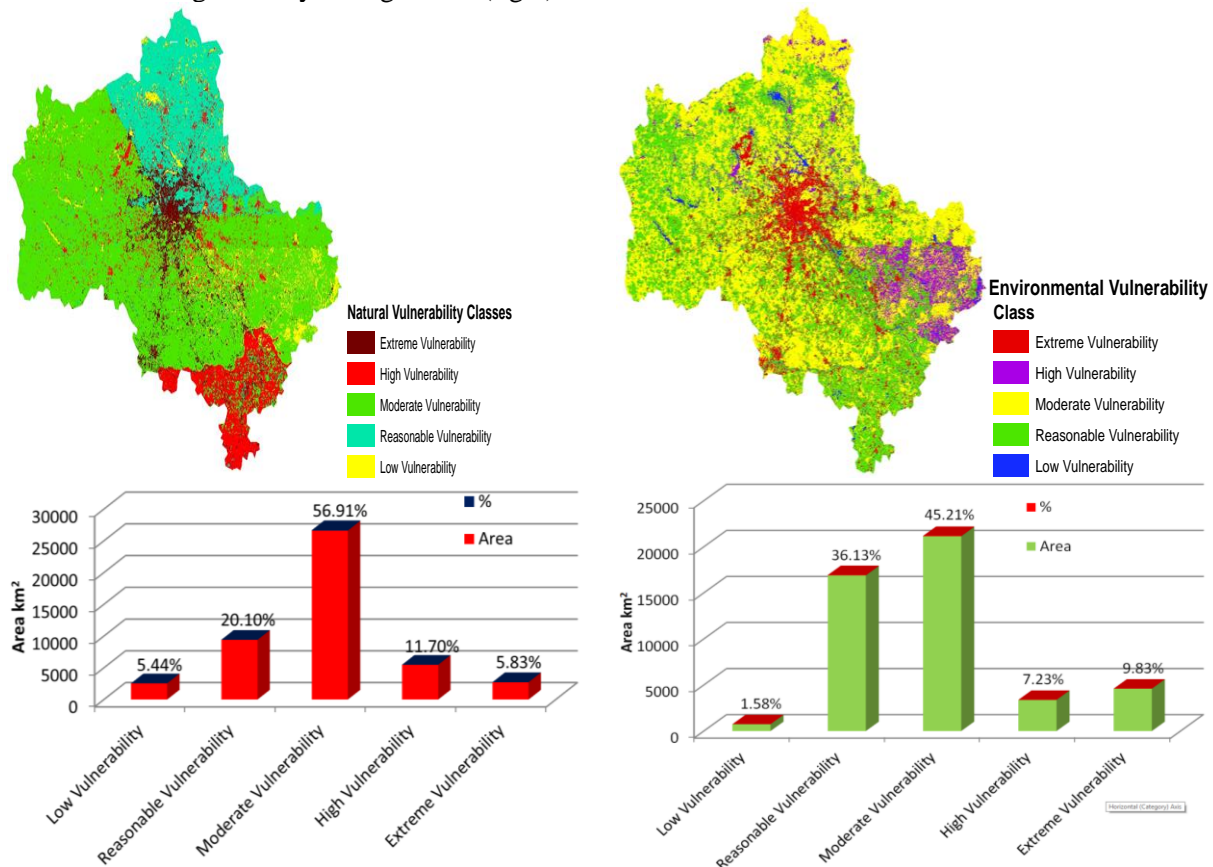


Figure 6. Natural and environmental vulnerability map.

4.4. Environmental vulnerability

Environmental vulnerability map is more sensitive than natural vulnerability. In environmental vulnerability around 46% area under moderate vulnerability zone but high and extreme vulnerability is higher than natural vulnerability. Here 7.23% area under high vulnerability and 9.83% under extreme vulnerability. Reasonable vulnerability is 36.13% and low vulnerability is 1.58%. Low vulnerability is present in river and water bodies, reasonable vulnerability present in wasteland and some parts in vegetation. Maximum study area has been under moderate vulnerability, which is present in vegetation and close to wetland and costal line. High vulnerability is present in close to river and its channels (fig.6). As study area is in north part of the Asia so maximum time of the year it is cover with ice, with harsh climatic condition. In winter only airways are the only way of approaching this area but in Summer Rivers also provide transportation facility. Here land use/cover classes and there convergent or encroachment induced by extreme cold and tough climatic condition in the study area. In extreme cold condition maximum areas convert in wasteland, where land has been unfertile. But in summer session ice has been melt and maximum land convert into wetland, forest and vegetation area etc.

5. Conclusion

Based on multi-temporal Landsat images, we determined that there was significant expansion of anthropogenic land cover in the Moscow. Analysis revealed that the area of anthropogenic land cover

was increased, resulting in a substantial reduction in natural land cover. The inundation maps can be overlaid on land use/cover maps to find out the extent of submergence of different land use/cover areas. By contrast, arable land declined by 10% due to occupation by urbanization and industrialization. It is necessary to incorporate the elevation levels for new settlements areas under the town planning acts so that human life and property are saved from natural hazards. The run-up levels can be used as guidance to determine safe locations of settlements from river basin. Vulnerability scenarios are useful for exploring uncertainties in vulnerability assessment on a regional basis, some regions show equal vulnerability to all scenarios, while other regions show different responses. This is an indicator for where we can be more or less uncertain about the future. Furthermore, it helps in indicating how society and policy can have an important role to play in future development pathways. The mapping, monitoring and modelling of land use/cover in such a vast territory as Moscow region could also contribute to the study of global environmental change.

6. References

- [1] Tabak N M, Laba M and Spector S 2016 Simulating the Effects of Sea Level Rise on the Resilience and Migration of Tidal Wetlands along the Hudson River *PLoS One* **11(4)** 0152437 DOI:10.1371/journal.pone.0152437
- [2] Boori M S and Ferraro R R 2015 Global Land Cover classification based on microwave polarization and gradient ratio (MPGR) *Geo-informatics for Intelligent Transportation* **71** 17-37 DOI:10.1007/978-3-319-11463-7-2
- [3] Yang Z, Wang T, Voisin N and Copping A 2015 Estuarine response to river flow and sea-level rise under future climate change and human development *Estuarine, Coastal and Shelf Science* **156** 19-30
- [4] McGranahan G, Balk D and Anderson B 2017 The rising tide: assessing the risks of climate change and human settlements in low elevation coastal zones *Environ. Urban.* **19(1)** 17-37
- [5] Sun X, Li Y and Zhu X 2015 Integrative assessment and management implications on ecosystem services loss of coastal wetlands due to reclamation *J. Clean. Prod.*
- [6] Cui L, Ge Z, Yuan L and Zhang L 2015 Vulnerability assessment of the coastal wetlands in the Yangtze Estuary, China to sea-level rise *Estuarine, Coastal and Shelf Science* **156** 42-51
- [7] Sweet W V and Park J 2014 From the extreme to the mean: Acceleration and tipping points of coastal inundation from sea level rise *Earth's future* **2(12)** 579-600
- [8] Yabuki H, Park H, Kawamoto H, Suzuki R, Razuvaev V N, Bulygina O N and Ohata T 2011 Baseline Meteorological Data in Siberia (BMDS) Version 5.0, RIGC, JAMSTEC, Yokosuka, Japan *Distributed by CrDAP, Digital Media*
- [9] Rotzoll K and Fletcher C H 2013 Assessment of groundwater inundation as a consequence of sea level Rise *Nature Climate Change* **3** 477-481
- [10] Shalaby A and Tateishi R 2007 Remote sensing and GIS for mapping and monitoring land cover and land-use changes in the Northwestern coastal zone of Egypt *Appl. Geogr.* **27(1)** 28-41
- [11] Choudhary K, Boori M S and Kupriyanov A 2017 Mapping and evaluating urban density patterns in Moscow, Russia *Computer Optics* **41(4)** 528-534 DOI: 10.18287/2412-6179-2017-41-4-528-534
- [12] Tian G and Wu J 2015 Comparing urbanization patterns in Guangzhou of China and Phoenix of the USA: The Influences of Roads and Rivers *Ecol. Indic.* **52** 23-30
- [13] Thakur A K, Sing S and Roy P S 2008 Orthorectification of IRS-P6 LISS IV data using Landsat ETM and SRTM datasets in the Himalayas of Chamoli district *Uttarakhand. Curr. Sci.* **95** 1459
- [14] Thomlinson J R, Bolstad P V and Cohen W B 1999 Coordinating methodologies for scaling land cover classifications from site-specific to global: steps toward validating global map products *Remote Sens. Environ.* **70(1)** 16-28
- [15] Choudhary K, Boori M S and Kupriyanov A 2017 Spatio-temporal analysis through remote sensing and GIS in Moscow region, Russia *CEUR Workshop Proceedings* **1901** 42-46
- [16] Courchamp F, Hoffmann B D, Russell J C, Leclerc C and Bellard C 2014 Climate change, sea-level rise, and conservation: keeping island biodiversity afloat *Trends in Ecology & Evolution* **29(3)** 127-130

- [17] Boori M S, Choudhary K, Kupriyanov A and Kovelskiy V 2015 Four decades urban growth and land use change in Samara Russia through remote sensing and GIS techniques *SPIE Remote Sensing and Image Formation* **9817** 01-07 DOI:10.1117/12.2227992
- [18] Barbosa C C F 1997 Álgebra de mapas e suas aplicações em Sensoriamento Remoto Geoprocessamento *Dissertação (Mestrado em Sensoriamento Remoto) – Instituto Nacional de Pesquisas Espaciais INPE* **111**

Acknowledgements

This work was partially supported by the Ministry of education and science of the Russian Federation; by the Russian Foundation for Basic Research grants (#16-41-630761; #16-29-11698, #17-01-00972).